

Modification of Tube Size and Shape in a Helical Tubuland Inclusion Lattice formed by a New Family of Diol Hosts: Syntheses and Crystal Structures†

Ian G. Dance,* Roger Bishop,* Stephen C. Hawkins, Tony Lipari, Marcia L. Scudder, and Donald C. Craig

School of Chemistry, University of New South Wales, Kensington, New South Wales 2033, Australia

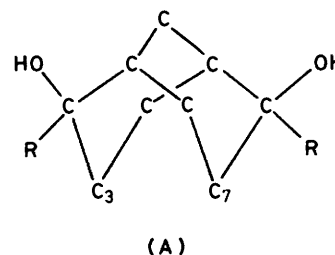
The four diols *exo*-2,*exo*-6-dihydroxy-2,6-dimethylbicyclo[3.3.1]nonane (1), *syn*-2,*syn*-7-dihydroxy-2,7-dimethyltricyclo[4.3.1.1^{3,8}]undecane (2), *anti*-2,*anti*-7-dihydroxy-2,7-dimethyltricyclo[4.3.1.1^{3,8}]undecane (3), and *syn*-2,*syn*-8-dihydroxy-2,8-dimethyltricyclo[5.3.1.1^{3,9}]dodecane (4) have been synthesised by stereospecific reaction of mercury(II) acetate or methyl-lithium with the diolefin or diketone precursor. All four compounds adopt the same crystal structure type, in which diol molecules connect a hexagonal array of hydrogen-bonded spines, in space group *P*3₁21, creating helical tubular cavities in the host crystal. However, different bridges between the two hydroxy functions of the host molecules cause substantial differences in the dimensions of the crystal lattice and in the shapes and unobstructed cross-sectional areas A^{un} of the tubes. For (1)–(4) respectively, unit-cell volumes are 897, 1 042, 858, and 1 150 Å³, and A^{un} values are 22.4, 30.2, 4.7, and 34.7 Å².

We have previously reported^{1,2} on the crystal structure of the bicyclic diol *exo*-2,*exo*-6-dihydroxy-2,6-dimethylbicyclo[3.3.1]nonane (1), which forms inclusion complexes with ethyl acetate and other guest molecules. In crystals of the inclusion complex of (1) with ethyl acetate [stoichiometry (1)₃·EtOAc] the guest molecule is disordered and mobile in helical tubes which have an approximately triangular cross-section. This crystal structure is based on tight spiral spines of hydrogen bonds, ...O–H...O–H...O–H...: the diol molecules radiate from and interconnect these spines, such that there are six spines surrounding each tube in a hexagonal pattern as shown in Figure 1. Both the spines and the tubes surround crystallographic three-fold screw axes in the trigonal space group *P*3₁21. Diol molecules hydrogen-bonded in sequence form double helices (pitch 2*c*) around the tubes, the walls of which are lined only by hydrocarbon hydrogen atoms.

This is a multimolecular inclusion complex, distinct from unimolecular inclusion complexes formed by host molecules such as crown ethers or cryptands, and distinct also from multimolecular inclusion complexes such as those formed by quinols and 4-*p*-hydroxyphenyl-2,2,4-trimethylchroman (Dianin's compound) which are based on cycles rather than helices of hydrogen bonds.^{3,4} The new and unique host lattice type adopted by crystalline (1) and its ethyl acetate complex is hereafter referred to as the 'helical tubuland' structure type. All helical tubes in each crystal possess the same chirality: spontaneous resolution of the host occurs in the crystallisation of this structure type, which therefore is an instance of the relatively rare conglomerate classification of Jacques *et al.*⁵

We are interested in the generality of occurrence of this helical tubuland crystal structure, with respect to variation of both the host molecule and the guest molecule, and in the utility of the inclusion and resolution phenomena associated with crystallisation of this structure. The primary objectives are (i) to ascertain the properties of the host molecule necessary for the

formation of this trigonal inclusion crystal structure, and (ii) to modify the size and the shape of the volume available to the guest species. In the essential core framework (A) of the diol host



(1) the distance between C-3 and C-7 is approximately that of an ethano bridge, and therefore we have examined potential host molecules with such a bridge in this position. We have reported briefly that the diol *syn*-2,*syn*-7-dihydroxy-2,7-dimethyltricyclo[4.3.1.1^{3,8}]undecane‡ (2) crystallises from ethyl acetate with the trigonal host structure of (1)₃·EtOAc, but crystallises from benzene as a different multimolecular inclusion complex with a tetragonal lattice, in which benzene guests are included in tight cavities and are unable to move between them.⁶

We have now determined that the diols *anti*-2,*anti*-7-dihydroxy-2,7-dimethyltricyclo[4.3.1.1^{3,8}]undecane (3) and *syn*-2,*syn*-8-dihydroxy-2,8-dimethyltricyclo[5.3.1.1^{3,9}]dodecane (4) also crystallise with the helical tubuland crystal lattice. The set of four host diols (1)–(4) now known to adopt this structure possesses two structural variables: one is the bridge connecting C-3 and C-7 of (A), a bridge which is absent in (1), ethano in (2) and (3), and propano in (4); the other is the configuration of the two hydroxy functions which are *exo*,*exo* in the bicyclic system (1), *anti*,*anti* in (3), and *syn*,*syn* in (2) and (4). These variations cause substantial modification of the guest space in the host lattice, in fulfilment of objective (ii).

In this paper we report details of the syntheses and crystal structure determinations for these four compounds, and outline

† Supplementary data available (SUP 56555, 6 pp.): thermal parameters, calculated H co-ordinates. For details of Supplementary Publications see Instructions for Authors (*J. Chem. Soc., Perkin Trans. 2*, 1986, Issue no. 1). Structure factor tables are available from the editorial office on request.

‡ Hydroxy groups are designated *syn* or *anti* with respect to the larger of the bridges across the molecular two-fold or pseudo-two-fold axis.

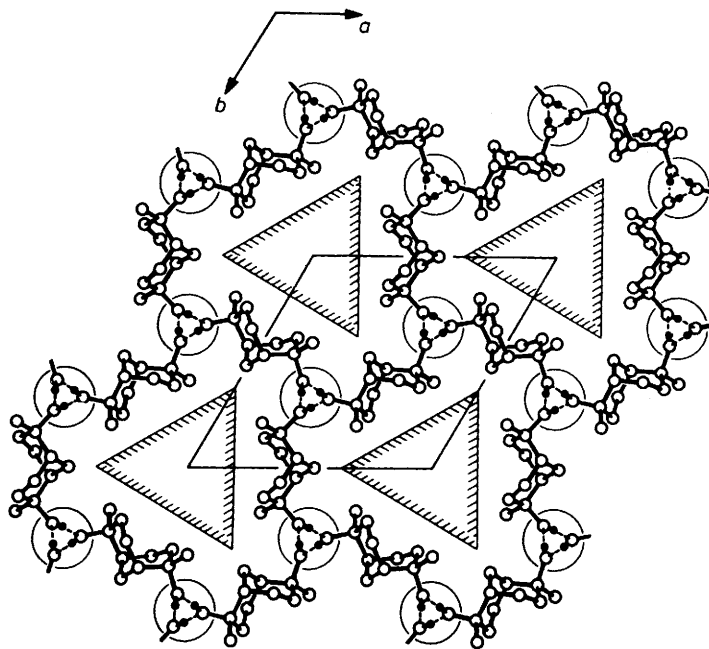
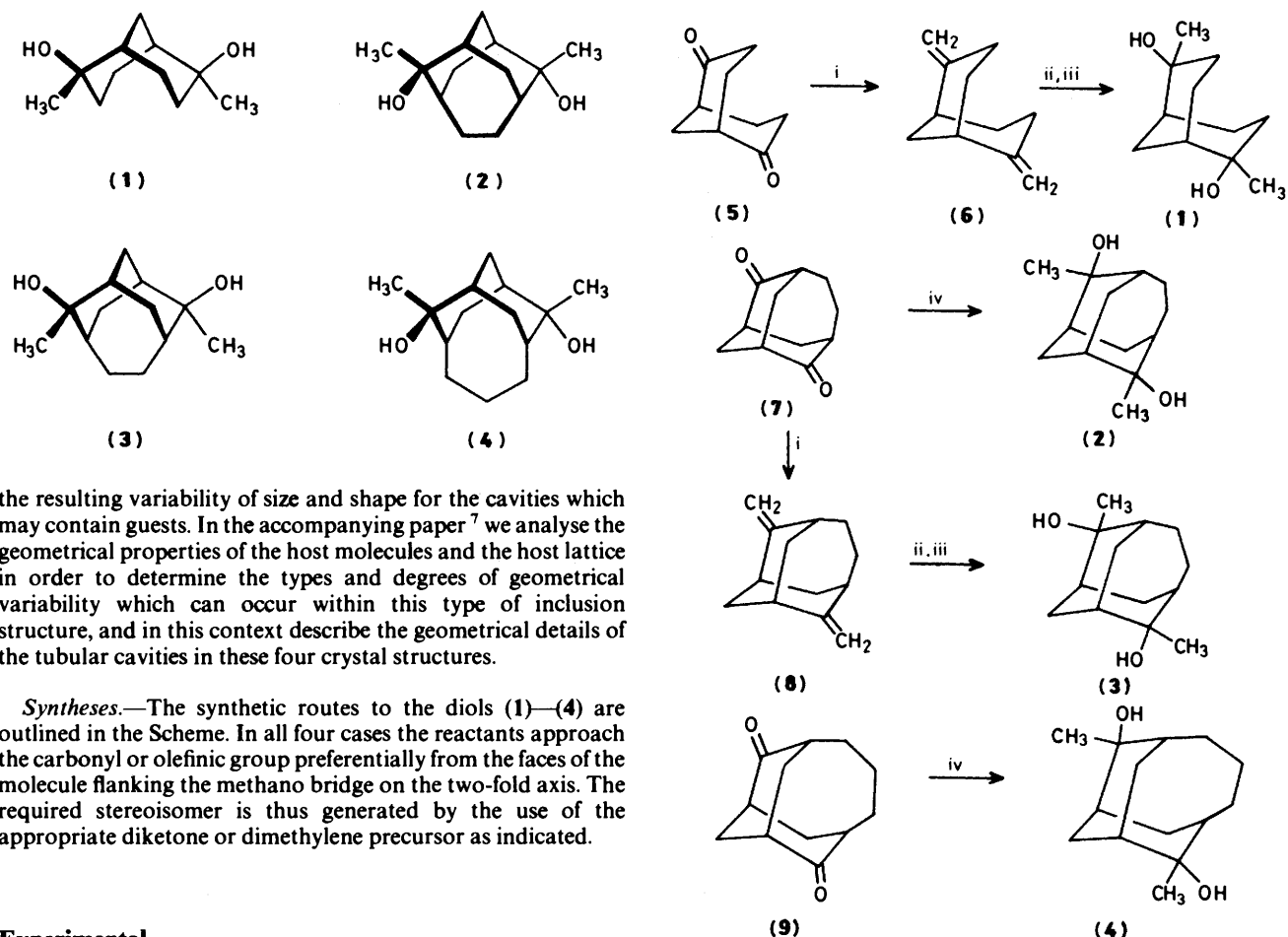


Figure 1. Projection view, parallel to the three-fold screw axes, of the diol host network in (1): the filled circles and dotted lines represent OH hydrogen atoms and hydrogen bonds, respectively; other hydrogen atoms are omitted for clarity. The hydrogen-bonded spines are circled, and the tubes are outlined as triangles



the resulting variability of size and shape for the cavities which may contain guests. In the accompanying paper⁷ we analyse the geometrical properties of the host molecules and the host lattice in order to determine the types and degrees of geometrical variability which can occur within this type of inclusion structure, and in this context describe the geometrical details of the tubular cavities in these four crystal structures.

Syntheses.—The synthetic routes to the diols (1)—(4) are outlined in the Scheme. In all four cases the reactants approach the carbonyl or olefinic group preferentially from the faces of the molecule flanking the methano bridge on the two-fold axis. The required stereoisomer is thus generated by the use of the appropriate diketone or dimethylene precursor as indicated.

Experimental

N.m.r. spectra (¹H 100 MHz and ¹³C 25.1 MHz) were recorded with a JEOL FX-100 spectrometer; chemical shifts are reported relative to internal SiMe₄. The substitution of carbon

Scheme. Reagents: i, Ph₃P=CH₂; ii, Hg(OAc)₂-H₂O; iii, NaBH₄-NaOH; iv, CH₃Li

atoms was determined by off-resonance decoupling. M.p.s were obtained with a Kofler instrument and exact masses were determined with an A.E.I. MS12 (electron impact) or MS9 (chemical ionisation) spectrometer.

exo-2,exo-6-Dihydroxy-2,6-dimethylbicyclo[3.3.1]nonane (1).—Bicyclo[3.3.1]nonane-2,6-dione (5) was converted into 2,6-dimethylenebicyclo[3.3.1]nonane (6) as described previously.⁸

(a) Mercury(II) acetate (23.90 g, 0.075 mol) in water (100 ml) and tetrahydrofuran (THF) (100 ml; freshly distilled from LiAlH₄) was stirred at room temperature,⁹ then a solution of 2,6-dimethylenebicyclo[3.3.1]nonane (4.81 g, 0.0325 mol) in THF (25 ml) was added. The yellow colour was discharged after about 1 min, but stirring was continued for 25 min. A solution of sodium hydroxide (3M; 75 ml) was added, followed by a further 75 ml (also 0.5M in NaBH₄). THF was evaporated off, and the solution was extracted continuously with ethyl acetate for 8 days. On cooling, much of the product crystallised from solution, but solvent was evaporated off and the entire residue recrystallised from acetonitrile to give the *diol* (3.97 g, 66%), m.p. 182—183 °C. Further recrystallisation to remove traces of borate impurities gave material with m.p. 189—191 °C (preceded by sublimation, sealed capillary) (Found: C, 71.4; H, 11.1. C₁₁H₂₀O₂ requires C, 71.7; H, 10.9%); ν_{\max} (paraffin mull) 3 340 (s), 1 235 (m), 1 095 (m), 1 075 (m), 1 020 (m), 980 (m), 915 (m), and 880 (m) cm⁻¹; δ_{H} [(CD₃)₂SO] 1.06 (s, 6 H), 1.2—1.9 (m, 12 H), and 3.88 (s, 2 H, exchanged with D₂O); δ_{C} [(CD₃)₂SO] 23.7 (t), 25.4 (t), 29.5 (q), 34.4 (t), 39.0 (d), and 70.0 (s).

(b) The reaction was carried out as in (a) to the addition of the alkaline NaBH₄ solution. After stirring overnight at room temperature, the THF layer was separated, and the highly insoluble product extracted thoroughly with THF (6 × 400 ml). The combined extracts were dried (Na₂SO₄), filtered, and evaporated and the crude product was recrystallised from ethyl acetate to give the *diol-ethyl acetate complex*¹ (4.48 g, 57% based on the analytical stoichiometry) [Found: C, 69.3; H, 10.6. (1)₃·EtOAc (C₃₇H₆₈O₈) requires C, 69.3; H, 10.7%]; ν_{\max} (paraffin mull) peaks as in (a), plus ethyl acetate absorptions at 1 745, 1 230, and 1 030 cm⁻¹; δ_{H} [(CD₃)₂SO] peaks as in (a) plus 1.17, 1.99, and 4.03; δ_{C} [(CD₃)₂SO] peaks as in (a) plus 14.0, 20.7, 59.6, and 170.2.

Tricyclo[4.3.1.1^{3,8}]undecane-2,7-dione (7).—Sodium hydride (1.80 g of 50% suspension; 37 mmol) and dry, freshly distilled 1,2-dimethoxyethane (15 ml) were stirred under dry N₂, and dimethyl 2,6-dihydroxybicyclo[3.3.1]nona-2,6-diene-3,7-dicarboxylate¹⁰ (3.0 g, 11.2 mmol) in 1,2-dimethoxyethane (20 ml) was added dropwise. The mixture was distilled to remove solvent (10 ml), and an excess of freshly distilled 1,2-dibromoethane (20 g) was added. More solvent (10—15 ml) was distilled off, and the mixture was heated at an oil-bath temperature of 110—120 °C for 20 h, before cooling and filtering to remove the precipitate of sodium bromide. This was washed with hot chloroform and the combined filtrate and washings were evaporated at reduced pressure. The residual yellow oil was dissolved in a little diethyl ether and cooled. Much of the product crystallised and was filtered off. Further material was obtained after column chromatography on alumina to give dimethyl 2,7-dioxotricyclo[4.3.1.1^{3,8}]undecane-3,6-dicarboxylate (0.76 g, 23%), m.p. 198 °C (from diethyl ether) (lit.,¹¹ 197—198 °C).

The diester (1.0 g, 3.4 mmol), mixed with acetic acid (6 ml) and 5M-HCl (4 ml), was refluxed overnight. Solvents were evaporated off to yield 2,7-dioxotricyclo[4.3.1.1^{3,8}]undecane-3,6-dicarboxylic acid (0.86 g, 95%), m.p. 289—292 °C (decomp.) (from acetone) [lit.,¹¹ 288—290 °C (decomp.)].

The diacid (1.06 g, 4.0 mmol) was placed in a sublimation vessel fitted with a cold finger, and heated at 280 °C and 0.5 atm.

Decarboxylation and sublimation were complete within 5 min, to yield the *diketone* (0.61 g, 86%), m.p. 302—303 °C (from ether—light petroleum) (lit.,¹² 303—304 °C); ν_{\max} (paraffin mull) 1 710 (s) cm⁻¹; δ_{H} (CDCl₃) 1.6—2.0 (m, 6 H), 2.0—2.4 (m, 4 H), 2.6—2.8 (m, 2 H), and 2.8—3.0 (m, 2 H); δ_{C} (CDCl₃) 26.4 (t), 32.5 (t), 35.3 (t), 43.9 (d), 46.4 (d), and 214.9 (s).

syn-2, syn-7-Dihydroxy-2,7-dimethyltricyclo[4.3.1.1^{3,8}]undecane (2).—Dry bromomethane was slowly bubbled into a stirred suspension of thin slices of lithium (60 mg, 8.4 mmol) in anhydrous ether (20 ml) at -10 °C under argon until the metal dissolved (ca. 15 min). The diketone (7) (220 mg, 1.4 mmol) in dry ether (20 ml) was added dropwise, immediately producing a white precipitate. Stirring was continued for 2 h at -10 °C, and then overnight at room temperature, before cautious addition of damp ether, then water, and extraction of the mixture with ether. Evaporation of the dried ethereal extracts gave a white powder, analysis of which by t.l.c. and g.l.c. (SE-30; 230 °C) showed it to be ca. 95% *syn, syn*-diol (2) and 5% *anti, syn*-isomer, with no *anti, anti*-diol (3) present. (The use of higher reaction temperatures decreased the proportion of the required isomer.) One recrystallisation from benzene gave (2) in the form of an *inclusion complex*⁶ [Found: C, 75.7; H, 10.7. (2)₄·C₆H₆ (C₅₈H₈₄O₈) requires C, 75.8; H, 10.3%]. Recrystallisation of this from ether and warming under reduced pressure gave the solvent-free *diol* (215 mg, 83%), m.p. 146—148 °C (Found: [M - 15]⁺, 195.1406. C₁₂H₁₉O₂ requires M - 15, 195.1385); ν_{\max} (paraffin mull) 3 240 (s), 1 125 (m), 1 100 (s), 940 (m), and 880 (m) cm⁻¹; δ_{H} (CDCl₃) 1.40 (s, 8 H, two CH₃ plus two OH, integration 6 H after exchange with D₂O) and 1.4—2.2 (m, 14 H); δ_{C} (CDCl₃) 27.9 (t), 30.3 (q), 32.5 (t), 32.7 (t), 40.0 (d), 43.4 (d), and 75.2 (s); *m/z* 195 (89%, [M - 15]⁺), 192 (11), 177 (19), 174 (17), 159 (17), 149 (24), 145 (14), 133 (12), 131 (11), 119 (16), 117 (11), 107 (21), 105 (23), 93 (36), 91 (26), 81 (27), 79 (27), and 43 (100).

2,7-Dimethylenetricyclo[4.3.1.1^{3,8}]undecane (8).—The diketone (7) (0.43 g, 2.42 mmol) was added to a stirred solution of methylenetriphenylphosphorane (6.04 mmol) in dry Me₂SO under dry nitrogen, as in the Corey method¹² for the Wittig reaction. After heating for 2 h at 75 °C, the cooled mixture was worked up in the usual manner with water and ether. The crude product was eluted with pentane through a short column of neutral alumina. Evaporation left the *diene* (0.31 g, 74%) as a waxy solid, m.p. 55—60 °C (Found: M⁺, 174.1389. C₁₃H₁₈ requires M, 174.1409); ν_{\max} (paraffin mull) 3 060 (m), 1 640 (s), 1 020 (w), 885 (s), and 690 (w) cm⁻¹; δ_{H} (CDCl₃) 1.5—1.8 (m, 8 H), 1.8—2.1 (m, 2 H), 2.4—2.6 (m, 2 H), 2.6—2.8 (m, 2 H), and 4.64 (s, 4 H); δ_{C} (CDCl₃) 33.3 (t), 37.6 (d), 38.7 (t), 39.5 (t), 40.7 (d), 106.8 (t), and 157.0 (s); *m/z* 174 (80%, M⁺), 159 (27), 145 (36), 131 (48), 117 (43), 105 (56), 91 (100), and 79 (52).

anti-2, anti-7-Dihydroxy-2,7-dimethyltricyclo[4.3.1.1^{3,8}]undecane (3).—The diene (8) (150 mg, 0.86 mmol) in THF (3 ml; freshly distilled from LiAlH₄) was added to a stirred mixture of mercury(II) acetate (0.55 g, 1.73 mmol) in distilled THF (5 ml) and water (5 ml). Within 20 min the yellow colour had been discharged, and stirring was continued for a further 1 h. A solution of sodium hydroxide (3M; 2 ml) was added, followed by a further 2 ml (also 0.5M in NaBH₄). After 20 min the THF was evaporated off and the aqueous residue extracted continuously with ethyl acetate for 4 days. Evaporation of the dried solution gave a white powder (100 mg, 55%), analysis of which by t.l.c. and g.l.c. showed it to be ca. 70% of the required *anti, anti*-diol (3) plus amounts of both the other isomers. Recrystallisation twice from acetonitrile gave the pure *diol* (69 mg, 38%), m.p. 245—247 °C (sealed capillary). This isomer is only sparingly soluble in most common solvents (Found: C, 74.2; H, 10.5. C₁₃H₂₂O₂

Table 1. Crystallographic details for (1)–(4)

	(1)	(2)	(3)	(4)
Formula	$C_{11}H_{20}O_2 + x(C_4H_8O_2)$	$C_{13}H_{22}O_2 + x(C_4H_8O_2)$	$C_{13}H_{22}O_2 + x(C_4H_8O_2)$	$C_{14}H_{24}O_2 + x(C_6H_6)$
Formula mass ($x = 0$)	184.3	210.3	210.3	224.3
Crystal description		Needles {001}{010}{100} {110}	{100}{010}{0-11}{101} {1-10}{1-1-1}	(00-1)(011)(-101) (1-11){1-10}{010}{100}
Space group	$P3_121$	$P3_121$	See text	$P3_121$
$a, b/\text{\AA}$	12.165	13.192 0(5)	11.905 6(5)	13.740 4(8)
$c/\text{\AA}$	7.001	6.913 7(2)	6.990 1(5)	7.030 1(5)
$V/\text{\AA}^3$	897.3	1 041.98(5)	858.05(7)	1 149.5(1)
Temp. ($^{\circ}\text{C}$)	21	21(1)	21(1)	21(1)
$D_{\text{obs.}}/\text{g cm}^{-3}$	1.10	1.19	1.22	<i>a</i>
Z	3	3	3	3
$D_{\text{calc.}}/\text{g cm}^{-3}$	1.02 ($x = 0$) 1.19 ($x = 1/3$)	1.01 ($x = 0$) 1.15 ($x = 1/3$)	1.22 ($x = 0$) 1.39 ($x = 1/3$)	0.97 ($x = 0$) 1.09 ($x = 1/3$)
Radiation, $\lambda/\text{\AA}$	Cu, 1.5418	Cu, 1.5418	Cu, 1.5418	Cu, 1.5418
μ/cm^{-1}		5.77 ($x = 1/3$)	7.01 ($x = 1/3$)	6.00
Crystal dimensions (mm)		0.52 \times 0.18 \times 0.22	0.16 \times 0.20 \times 0.35	0.19 \times 0.12 \times 0.50
Scan mode	$\theta/2\theta$	$\theta/2\theta$	$\theta/2\theta$	$\theta/2\theta$
$2\theta_{\text{max.}}$ ($^{\circ}$)		140	140	130
No. of intensity measurements		1 062	1 808	2 207
Criterion for observed reflection		$I/\sigma(I) > 3$	$I/\sigma(I) > 3$	$I/\sigma(I) > 3$
No. of independent observed reflections	633	694	1 345	695
No. of reflections (m) and variables (n) in final refinement	544, 63	596, 72	1 167, 204	584, 81
R	0.049 for $\sin\theta/\lambda > 0.3$ 0.087 for all data	0.041 for $\sin\theta/\lambda > 0.3$ 0.078 for all data	0.039 for $\sin\theta/\lambda > 0.3$ 0.046 for all data	0.038 for $\sin\theta/\lambda > 0.3$ 0.070 for all data
R_w	0.053	0.058	0.050	0.052
s	4.01	2.05	1.69	1.75
Max., mean, min. transmission coeffs.		0.91, 0.90, 0.83	0.91, 0.88, 0.82	0.93, 0.91, 0.84
Crystal decay		1 to 0.70	None	None
$F(000)$ ($x = 0$)	306	348	348	372

* A density measurement on a subsequent sample has given a high value (1.18 g cm^{-3}) which is under investigation.

requires C, 74.1; H, 10.6%; $v_{\text{max.}}$ (paraffin mull) 3 360 (s), 1 330 (w), 1 245 (w), 1 110 (w), 1 080 (s), 1 035 (m), 980 (w), 935 (m), 895 (w), and 890 (m) cm^{-1} ; $\delta_{\text{H}}[(\text{CD}_3)_2\text{SO}]$ 1.12 (s, 6 H), 1.23 (m, 2 H), 1.3–1.5 (m, 4 H), 1.65–1.85 (m, 4 H), 1.88 (m, 2 H), 2.07 (m, 2 H), and 3.90 (s, 2 H); $\delta_{\text{C}}[(\text{CD}_3)_2\text{SO}]$ 27.0 (q), 27.7 (t), 31.4 (t), 39.2 (d), 43.0 (d), 73.3 (s), and one signal (t) not resolved; m/z 210 ($< 1\%$, M^+), 195 (55), 192 (19), 177 (40), 174 (27), 159 (14), 149 (24), 145 (16), 119 (16), 117 (12), 107 (22), 105 (26), 93 (37), 91 (34), 81 (25), 79 (27), and 43 (100).

syn-2, syn-8-Dihydroxy-2,8-dimethyltricyclo[5.3.1.1^{3,9}]dodecane (4).—Methyl-lithium was prepared from bromomethane and lithium (6.3 mmol) in dry ether (15 ml) under the conditions just described. A solution of tricyclo[5.3.1.1^{3,9}]dodecane-2,8-dione (9)¹³ (300 mg, 1.56 mmol) in anhydrous THF (15 ml) was added at -10°C . The mixture was stirred at -10°C for a further 2 h, then at room temperature for 24 h before work-up. One recrystallisation from cyclohexane gave the *diol* (215 mg, 60%), m.p. 146.5–147 $^{\circ}\text{C}$ (chemical ionisation mass spectrometry with pyridine and hydrogen:¹⁴ found [$M + \text{H}/\text{pyridine}]^+$, 304.2266; $C_{19}H_{30}NO_2$ requires 304.2276; found: [$M - \text{H}/\text{pyridine}]^+$, 302.2176; $C_{19}H_{28}NO_2$ requires 302.2119); $v_{\text{max.}}$ (paraffin mull) 3 440 (s), 1 130 (m), 1 095 (s), 1 025 (m), 1 000 (m), 935 (s), 900 (w), and 875 (m) cm^{-1} ; $\delta_{\text{H}}(\text{CDCl}_3)$ 1.33 (s, 2 H, exchanged with D_2O), 1.37 (s, 6 H), 1.30–1.43 (m, 2 H), 1.48–1.54 (m, 2 H), 1.73–1.85 (m, 6 H), and 2.00–2.14 (m, 6 H); $\delta_{\text{C}}(\text{CDCl}_3)$ 23.1 (t), 28.0 (t), 29.8 (t), 31.2 (t), 34.1 (q), 38.2 (d), 39.4 (d), and 74.1 (s); m/z 224 ($< 1\%$, M^+), 209 (15), 206 (17), 191 (27), 188 (23), 173 (21), 165 (20), 163 (44), 147 (25), 131 (29), 129 (21), 111 (31), 107 (44), 105 (31), 95 (42), 93 (56), 91

(32), 81 (60), 79 (37), 71 (42), 67 (35), 55 (29), 43 (100), and 41 (37).

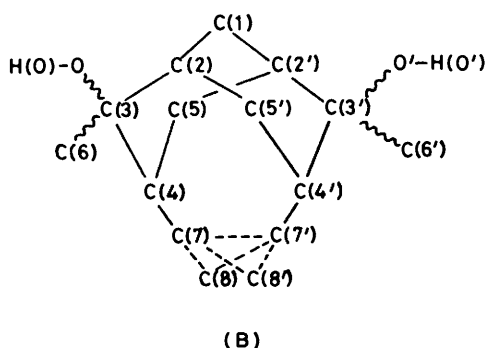
Crystallography.—Crystals for X-ray diffraction analysis were grown by evaporation at ambient temperature from ethyl acetate [for (1)–(3)] or benzene [for (4)]. When mechanically fractured, some crystals of (4) showed evidence of macroscopic occlusion of liquid benzene.

Diffraction analyses were made with Siemens [for (1)] and Enraf Nonius CAD4 [for (2)–(4)] diffractometers. Details of the crystals, the diffractometry conditions, the lattice dimensions, and the collection of intensity data are presented in Table 1. Evaluation of the crystal symmetry was important because in inclusion compounds the symmetry of the lattice of any guest molecules may be less than the symmetry of the host lattice, depending on the degree of guest occupancy and the degree of guest ordering. In (1), (2), and (4) no significant deviation from the symmetry of space group $P3_121$ was detectable: the discrepancy factor $R^1 = \sum_{hkl} \sum_i [I_i^{hkl} - I_m^{hkl}] / I_m^{hkl} [I_m^{hkl} = (\sum_i I_i) / m]$ for measurements of equivalent reflections in this space group was 1.8% for (2) (314 measurements of 141 multiply observed reflections) and 2.2% for (4) (1 576 measurements of 734 multiply observed reflections). The data do not permit differentiation of the enantiomorphic space groups $P3_121$ and $P3_221$. However, in the crystals of (3) the symmetry of the diffraction intensities was clearly less than trigonal, even though the lattice geometry was trigonal. The discrepancy factor R^1 for (3) in space group $P3_121$ was 11.7% for 1 234 measurements of 574 multiply observed reflections. In fact the diffraction intensity data for the crystal of (3) investigated

revealed only two-fold symmetry about [110]: R^1 for 524 measurements of 262 multiply observed reflections in this symmetry was 3.7%. The uncertainty about the lattice symmetry for (3) is discussed further with the refinement of the structure.

All four structures were readily solved by direct methods with the program MULTAN 80. Calculated positions were used for all hydrogen atoms except those of the OH groups which were first located on difference maps and then refined. Inspection of difference maps showed that the methyl hydrogen atoms were in the staggered conformation. They were therefore included at positions calculated for that conformation.

The crystallographic atom labelling scheme (B) is common to



the host molecules in (1), (2), (3), and (4) (each of which has crystallographic two-fold symmetry). Where structure (3) is treated in the lower symmetry lattice, one molecule (designated B) has exact two-fold symmetry; another, with pseudo-two-fold symmetry, has its two halves designated A and C. Atoms C(7) and C(7') constitute the ethano bridge of (2) and (3); in (4) the central carbon atom of the propano bridge is disordered across the two-fold axis, between C(8) and C(8'). Hydrogen atoms are labelled according to the carbon atoms to which they are bonded.

For each of (1), (2), (3), and (4), full-matrix, least-squares refinement was completed with the following protocol. All non-hydrogen atoms were refined with anisotropic thermal parameters. The methyl and methylene hydrogen atoms were included in calculated positions and were assigned isotropic temperature factors equivalent to those of the atoms to which they were bonded. The positions of the hydroxylic hydrogen atoms were determined from difference maps and then refined with isotropic temperature factors maintained equivalent to those of the corresponding oxygen atoms. All refinement was performed using restricted data with $\sin\theta/\lambda > 0.3$. In this way, the structures of the host molecules were not influenced by the existence or otherwise of guest molecules. At convergence, the residuals R were calculated for the complete data sets for comparison. The difference maps discussed were computed using the complete reflection data along with parameters resulting from refinement with restricted data. No corrections for anomalous dispersion or extinction were necessary.

Details specific to each crystal and to the possible occurrence and location of guest species are described in the following.

Refinement of structure (1). Refinement using data with $\sin\theta/\lambda > 0.3$ converged with $R = 0.049$; that with all data used was 0.087. The obvious disagreement of the low-angle data was evidence for the existence of a guest molecule. This was further supported by the existence of peaks in the final difference map up to $1.1 \text{ e } \text{\AA}^{-3}$. However, it was not possible to resolve this electron density into a meaningful representation of an ethyl acetate molecule. It was therefore assumed that the guest molecule, although present, was disordered or mobile.

Refinement of structure (2). Refinement of this structure converged with $R = 0.041$ for data with $\sin\theta/\lambda > 0.3$ and 0.078

for all data, indicating again that a guest molecule was contributing to the diffraction data. The largest peaks in the difference map were $0.8 \text{ e } \text{\AA}^{-3}$, but attempts to parameterise this residual electron density as an ethyl acetate molecule were unsuccessful. Since the peaks on the difference map were diffuse and poorly defined, it was concluded that the guest molecule was disordered.

Refinement of structure (3) The refinement of structure (3) was complicated, not only by the existence or otherwise of a guest molecule, but also by uncertainty about the diffraction symmetry of the measured reflection data (already noted). Although the measured density (1.22 g cm^{-3}) indicated that the host structure was empty ($D_{\text{calc.}}$ for one guest molecule per unit cell = 1.40 g cm^{-3} , $D_{\text{calc.}}$ for no guest molecule = 1.22 g cm^{-3}), the hypothesis that the presence of an ordered guest molecule in the host lattice could readily account for the observed lower symmetry of the diffraction data was entertained initially. In the early stages of the refinement, data with averaged values of multiple measurements for trigonal diffraction symmetry in space group $P3_121$ were used. Refinement converged with $R = 0.038$ using data with $\sin\theta/\lambda > 0.3$. When these parameters were used to calculate structure factors using data averaged according to the two-fold symmetry only (equivalent positions $x, y, z; y, x, -z$), the residual R was 0.063. Corresponding residuals using unaveraged data were 0.043 and 0.066, respectively. Residuals calculated for the lower symmetry data, in concentric shells radiating in 0.1 \AA^{-1} segments of $\sin\theta/\lambda$, ranged from 0.071 through 0.074 then down to 0.058 for the outermost shell. All these results indicated that very little scattering matter was unaccounted for by the host model only.

In a further attempt to find a reason for the lower diffraction symmetry of the data, refinement was continued with the only symmetry being a two-fold axis in the [110] direction (equivalent positions x, y, z and $y, x, -z$). Each diol atom was included in three positions (labelled A, B, C), except that C(1C) [= C(1A)] was omitted. With the data of two-fold symmetry restricted to $\sin\theta/\lambda > 0.3$, refinement converged with $R = 0.039$, and there were no significant systematic differences in the dimensions or locations of the diol molecules. The final difference map contained no peaks greater than $0.3 \text{ e } \text{\AA}^{-3}$. When refinement was continued using all reflections, the residual converged to 0.046. Thus refinement of the host structure either with imposed trigonal symmetry or with two-fold symmetry did not allow detection of significant additional electron density, and the reason for the lowered symmetry of the diffraction intensity has not been identified.

Refinement of structure (4). The central atom C(8) of the propano bridge was disordered across the two-fold axis. As a result, there were two alternate positions for each hydrogen atom on C(7), and both were included with half weight. At the conclusion of refinement, the residual R was 0.038 for data with $\sin\theta/\lambda > 0.3$ and 0.070 for all data. The largest peak on the final difference map was $0.6 \text{ e } \text{\AA}^{-3}$, indicating that any guest molecule present is highly disordered.

Refined atomic co-ordinates for the four structures are presented in Table 2.

Results

In the following description, the crystal structures of (1) *ex* ethyl acetate, (2) *ex* ethyl acetate, and (4) *ex* benzene are presented in space group $P3_121$. Differentiation from the enantiomorphic structure in space group $P3_221$ has not been possible. In the crystals of (3) *ex* ethyl acetate the symmetry of the diffraction intensities is less than trigonal (although the overall lattice geometry is still trigonal), and the only exact symmetry elements are two-fold axes normal to c at intervals of $c/2$. There are two crystallographically different molecules in (3). One (designated

Table 2. Positional parameters for structures (1)–(4), including only hydroxylic hydrogen atoms

	(1)				(3)		
	<i>x/a</i>	<i>y/b</i>	<i>z/c</i>		<i>x/a</i>	<i>y/b</i>	<i>z/c</i>
O	-0.263 0(2)	0.326 1(2)	0.223 6(3)	O(A)	-0.264 8(7)	0.316 5(7)	0.226 1(4)
C(1)	0.000 0	0.520 7(3)	0.166 7	O(B)	-0.315 8(7)	-0.580 8(7)	-0.440 0(3)
C(2)	-0.044 6(2)	0.425 1(2)	0.331 4(3)	O(C)	0.265 2(7)	0.581 0(7)	0.106 4(3)
C(3)	-0.162 4(2)	0.299 4(2)	0.269 1(3)	C(1A)	0.000 5(7)	0.516 7(7)	0.166 4(4)
C(4)	-0.139 0(2)	0.246 6(2)	0.085 7(4)	C(1B)	-0.516 9(14)	-0.516 9	-0.500 0
C(5)	-0.069 2(2)	0.346 3(2)	-0.069 0(0)	C(2A)	-0.042 5(7)	0.421 3(7)	0.334 5(4)
C(6)	-0.211 6(2)	0.199 1(3)	0.426 1(4)	C(2B)	-0.420 3(7)	-0.462 7(7)	-0.332 8(4)
HO	-0.285 5(35)	0.342 1(36)	0.298 6(65)	C(2C)	0.041 9(7)	0.463 6(7)	0.000 9(4)
				C(3A)	-0.160 9(7)	0.290 7(7)	0.274 8(4)
				C(3B)	-0.290 5(7)	-0.452 0(7)	-0.390 6(4)
				C(3C)	0.161 9(7)	0.452 3(7)	0.056 4(4)
				C(4A)	-0.138 6(7)	0.233 9(7)	0.091 9(4)
				C(4B)	-0.233 2(7)	-0.372 5(7)	-0.575 0(4)
				C(4C)	0.139 0(7)	0.372 5(7)	0.241 7(4)
				C(5A)	-0.076 0(7)	0.336 8(7)	-0.065 6(4)
				C(5B)	-0.336 9(7)	-0.413 0(7)	-0.732 0(4)
				C(5C)	0.076 5(7)	0.413 1(7)	0.398 9(4)
				C(6A)	-0.210 8(7)	0.193 9(7)	0.440 3(5)
				C(6B)	-0.193 7(7)	-0.405 1(7)	-0.226 2(5)
				C(6C)	0.210 9(7)	0.404 6(7)	-0.106 0(5)
				C(7A)	-0.067 7(7)	0.156 6(7)	0.120 3(5)
				C(7B)	-0.156 3(7)	-0.223 2(7)	-0.546 7(5)
				C(7C)	0.067 9(7)	0.224 3(7)	0.213 8(5)
				HO(A)	-0.271 5(44)	0.354 1(46)	0.318 8(77)
				HO(B)	-0.359 4(42)	-0.638 5(45)	-0.356 6(70)
				HO(C)	0.289 9(41)	0.630 2(42)	0.001 3(70)

	(2)		
	<i>x/a</i>	<i>y/b</i>	<i>z/c</i>
O	-0.241 9(1)	0.403 0(2)	0.133 5(3)
C(1)	0.000 0	0.714 4(3)	0.166 7
C(2)	-0.102 0(2)	0.596 3(2)	0.231 3(3)
C(3)	-0.149 1(2)	0.512 1(2)	0.059 2(3)
C(4)	-0.051 8(2)	0.495 7(2)	-0.035 5(3)
C(5)	0.060 6(2)	0.613 6(3)	-0.069 5(3)
C(6)	-0.203 9(2)	0.555 0(3)	-0.092 3(4)
C(7)	-0.028 1(3)	0.407 2(3)	0.067 3(4)
HO	-0.267 7(32)	0.358 7(34)	0.051 5(59)

	(4)		
	<i>x/a</i>	<i>y/b</i>	<i>z/c</i>
O	-0.236 1(1)	0.380 4(2)	0.225 6(3)
C(1)	0.000 0	0.322 2(3)	0.166 7
C(2)	-0.098 6(2)	0.337 5(2)	0.113 2(3)
C(3)	-0.142 9(2)	0.369 0(2)	0.290 0(3)
C(4)	-0.050 1(2)	0.477 4(2)	0.389 5(3)
C(5)	0.064 3(2)	0.480 5(2)	0.392 9(3)
C(6)	-0.189 9(2)	0.273 0(2)	0.434 1(4)
C(7)	-0.042 7(2)	0.588 5(2)	0.334 8(5)
C(8)	-0.046 0(5)	0.620 4(5)	0.146 8(9)
HO	-0.271 9(42)	0.385 4(37)	0.324 0(77)

B) has a crystallographic two-fold axis running through it, as do the molecules in (1), (2), and (4). In addition, the asymmetric unit of (3) also contains a molecule with a pseudo-two-fold axis: one half is designated A, the other C. In (4) the central CH₂ group of the propano bridge is disordered equally between two conformations either side of the two-fold axis through the remainder of the molecule.

Lattice and Tube Dimensions.—There are substantial differences in the dimensions of the crystal lattices (see Table 1). Although the *c* repeat distance is almost constant [ranging from 6.91 Å in (2) to 7.03 Å in (4)], the *a* lattice parameters and consequently the unit-cell volumes vary substantially: the cell volumes are 897 and 858 Å³ for (1) and (3), and 1 042 and 1 150 Å³ for (2) and (4), respectively. These lattice differences are due not to differences in interconnection lengths of the diol molecules but to variations in lattice packing arising from different diol shapes, explored in detail in the following paper.

The internal surface of the host tube is defined by the intersection of the van der Waals spheres of the hydrocarbon atoms which line the tube. The simplest representation of the tube size and shape is the projection of the unit cell along the tube axis with the internal van der Waals radii drawn. This defines the cross-sectional area which is unobstructed at all points along the tube, that is the cross-sectional area which is available to guest species of any length for translocation along the tube without steric impediment.

Figure 2 provides such projection views of the lattice

structure of each of the four crystals. It is clearly evident that the unobstructed cross-sectional area, A^{un} , differs substantially in size and shape. In (1) $A^{un} = 22.4 \text{ \AA}^2$, and is very close to triangular; in (2) the larger area $A^{un} = 30.2 \text{ \AA}^2$ is tri-lobed; in (3) ethano bridges of three host molecules intrude into the tube and reduce it to four thin unobstructed tubes with a total cross-section of only 4.7 Å²; the largest A^{un} of 34.7 Å² occurs in (4), and is hexa-lobed. In the following paper we examine the indentations in the walls of these four different tubes, with the conclusion that the tubes are not as different in capacity as indicated by the projection views of Figure 2.

Host Molecule Dimensions.—Bond distances and angles for the four host molecules are contained in Table 3. None of the bond distances or angles is anomalous. Contra-molecular dimensions, particularly the separation and angular relationship of the two C–OH groups, are important in evaluation of the diol molecules as connectors between the spines. Table 4 contains these dimensions. Despite the configurational differences between the set (1), (3) and the set (2), (4), the overall dimensions of the four hosts vary little. The contra-molecular O---O' separation ranges only between 5.54 and 5.68 Å, while the C(3)---C(3') and C(6)---C(6') separations differ by no more than 0.16 Å in 3.7 and 5.8 Å, respectively. The C(4)---C(4') separations are 3.14 Å for no bridge (1), 3.05 Å for the ethano bridge of (2) and (3), and 3.35 Å for the propano bridge of (4). The relative orientation of the two C–O bonds is

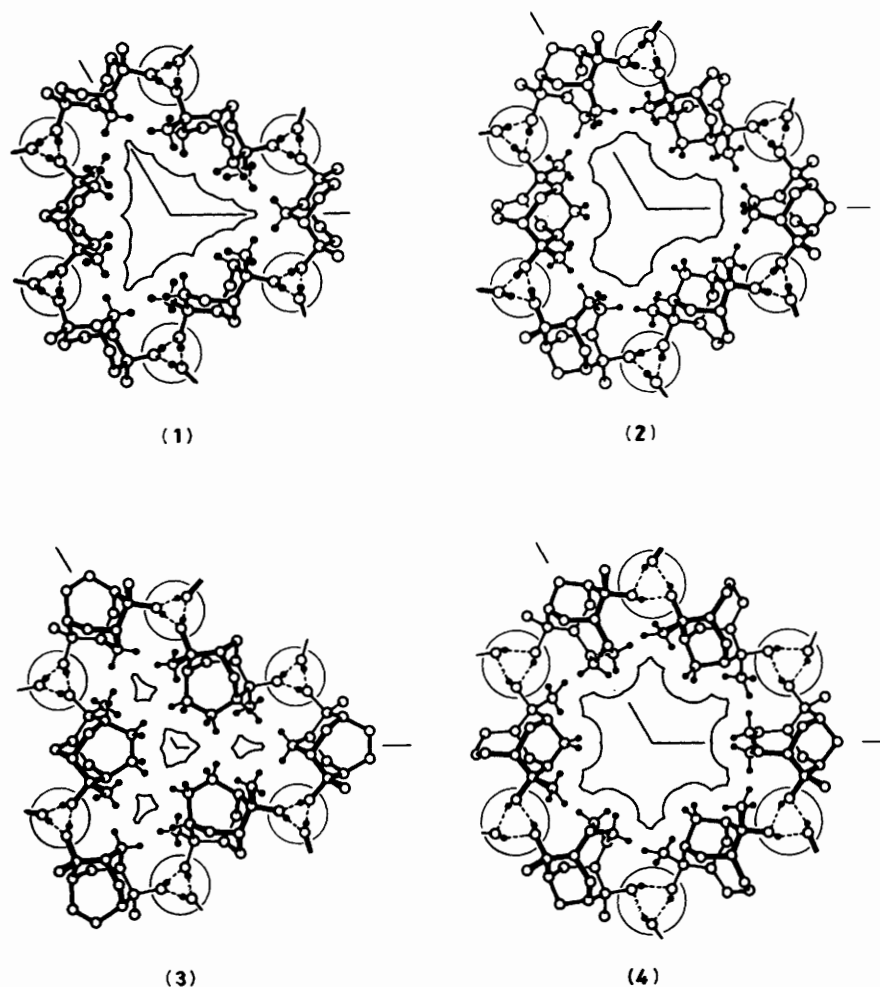


Figure 2. Comparative projections along the c axis of the diol molecules and the tubes they enclose in (1)–(4). The bond thickening signifies depth in individual molecules only because the helical characteristic is absent from these projections of the lattice. The tube boundaries are marked as the intersecting projected van der Waals spheres of the hydrogen atoms which line the tubes. All four diagrams are presented on the same scale. Significant hydrogen atoms are marked as filled circles, and the spines are circled

assessed by the $C(3')\text{---}C(3)\text{---}O$ angle, almost invariant at $122\text{--}126^\circ$, and by the $O\text{---}C(3)\text{---}C(3')\text{---}O'$ torsion angle which is smaller than 90° (73.5° , 79.0°) in the isomers (1) and (3) with the CH_2 bridge on the face *syn* to the $\text{C}\text{---}\text{OH}$ groups, and slightly larger than 90° (94.3° , 97.2°) in isomers (2) and (4) with the CH_2 bridge on the face of the molecule *anti* to the $\text{C}\text{---}\text{OH}$ functions.

The conclusion here is that the dimensions of the diols which are relevant to their role as connectors between the spines are very similar.

Guest Occurrence. In the crystals of (1), (2), and (4) the diffraction analysis has provided weak evidence for the presence but not for the positions of guest molecules in the tubes. This evidence appears as significant discrepancies between the observed and calculated (host) structure factors at $\sin\theta/\lambda < 0.3$ [$R = 0.157$ in (1), 0.146 in (2), and 0.124 in (4)], but difference-Fourier analyses yield low and flat residual electron densities (maxima 1.1 , 0.8 and 0.6 e \AA^{-3} , respectively) in the space group $P3_121$ of the host lattice, and are indicative of positional disorder and possibly low occupancy by guest molecules. It is important to recognise that the tube in this $P3_121$ structure type is pierced by lateral two-fold axes at intervals of $c/6$, *i.e.* *ca.* 1.2 \AA , and that it would be impossible for a small asymmetric guest such as ethyl acetate to conform with the symmetry of the $P3_121$ host lattice.

In the crystals of (3) the symmetry of the diffraction intensities

is less than trigonal, even though the lattice has trigonal geometry. Since the observed diffraction intensities represent the sum of contributions from the host and guest lattices, which need not have the same symmetry, and since the symmetry of the observed lattice *geometry* could be due to the host lattice only (the guest being included without strain in cavities), these initial results from crystals of (3) indicated the presence of an ordered array of ethyl acetate. However, as described in the Experimental section it was not possible to resolve any electron density greater than 0.3 e \AA^{-3} due to guest molecules. The structure factor residuals for data with $\sin\theta/\lambda < 0.3$ were 0.055 for the data averaged with trigonal symmetry, and 0.064 for the data with two-fold symmetry only. In (3) the tube dimensions are constricted to an extent that would not allow orientational disorder of ethyl acetate as guest, although disordered occupancy is possible. The capacity of the tubes in (3) to accommodate ethyl acetate is discussed in the accompanying paper.⁷ I.r. spectra indicated the presence of a small quantity of included ethyl acetate which was retained on warming (3).

Discussion

All other crystal structures for inclusion complexes formed by mono- or di-hydroxy hydrocarbon hosts contain globular inclusion cavities, not tubes,³ and thus the helical tubuland

Table 3. Bond lengths (Å) and interbond angles (°) for (1)–(4)

	(1)	(2)	(3)			(4)
			A	B	C	
C(1)–C(2)	1.532(3)	1.530(3)	1.533(4)	1.537(6)	1.514(5)	1.518(3)
C(2)–C(3)	1.547(3)	1.532(3)	1.545(4)	1.541(4)	1.550(4)	1.539(3)
C(3)–C(4)	1.525(3)	1.549(3)	1.530(5)	1.541(4)	1.547(3)	1.560(3)
C(4)–C(5)	1.529(4)	1.539(4)	1.535(4)	1.538(4)	1.535(5)	1.551(4)
C(5)–C(2')	1.528(3)	1.531(4)	1.532(4)	1.526(4)	1.536(4)	1.535(3)
C(4)–C(7)		1.527(4)	1.541(5)	1.552(5)	1.541(5)	1.528(4)
C(7)–C(7')		1.517(6)	1.544(5)	1.528(9)		
C(7)–C(8)						1.400(7)
C(7)–C(8')						1.553(7)
C(3)–O	1.450(3)	1.439(3)	1.456(4)	1.449(4)	1.449(4)	1.438(3)
C(3)–C(6)	1.525(4)	1.533(3)	1.528(4)	1.522(4)	1.510(5)	1.527(4)
O–HO	0.67(5)	0.76(5)	0.81(6)	0.85(5)	0.89(5)	0.87(6)
C(2)–C(1)–C(2')	108.8(2)	109.3(3)	109.5(2)	108.5(3)		108.5(3)
C(1)–C(2)–C(3)	109.8(1)	110.1(2)	109.7(2)	110.2(5)	110.6(2)	110.2(2)
C(1)–C(2)–C(5')	108.2(2)	108.1(2)	107.2(2)	107.5(5)	108.3(2)	108.2(2)
C(3)–C(2)–C(5')	116.3(2)	114.9(2)	114.9(2)	115.8(2)	114.9(2)	117.7(2)
C(2)–C(3)–C(4)	112.2(2)	111.5(2)	113.4(2)	112.8(2)	112.1(2)	112.4(2)
C(2)–C(3)–O	108.0(2)	106.4(2)	107.1(2)	107.8(2)	107.5(2)	106.0(2)
C(4)–C(3)–O	105.4(2)	111.2(2)	104.6(2)	104.2(2)	104.1(2)	112.6(2)
C(3)–C(4)–C(5)	114.2(2)	111.8(2)	111.7(2)	111.4(2)	111.7(2)	111.5(2)
C(4)–C(5)–C(2')	114.8(2)	115.5(2)	114.1(2)	114.7(2)	114.7(2)	119.0(2)
C(3)–C(4)–C(7)		114.3(2)	115.1(2)	115.1(3)	115.1(3)	117.0(2)
C(5)–C(4)–C(7)		112.4(2)	112.1(3)	111.8(2)	112.1(3)	114.6(2)
C(4)–C(7)–C(7')		119.8(1)	119.0(3)	119.3(2)	118.9(2)	
C(4)–C(7)–C(8)						123.6(3)
C(4)–C(7)–C(8')						119.6(3)
C(7)–C(8)–C(7')						121.1(4)
C(4)–C(3)–C(6)	110.6(2)	109.8(2)	112.8(2)	112.6(2)	112.4(3)	108.5(2)
C(2)–C(3)–C(6)	112.8(2)	111.0(2)	111.7(2)	112.1(3)	113.0(2)	110.4(2)
O–C(3)–C(6)	107.4(2)	106.9(2)	106.6(2)	106.7(2)	107.2(2)	106.8(2)
C(3)–O–HO	114(3)	109(2)	105(3)	114(3)	109(3)	109(3)

Table 4. Selected contra-molecular dimensions for (1)–(4)

Dimension	Compound			
	(1)	(2)	(3)	(4)
O---O' (Å)	5.60	5.55	5.53	5.68
C(3)---(3') (Å)	3.71	3.71	3.66	3.82
C(4)---(4') (Å)	3.14	3.04	3.05	3.35
C(6)---(6') (Å)	5.75	5.88	5.79	5.88
C(3')---(3)–O (°)	126.1	122.3	124.8	123.0
O–C(3)---(3')–O' (Å)	73.5	94.3	78.9	97.2
			124.7	
			124.6	
			79.1	

crystal structure described here is unique among multimolecular inclusion complexes. The host structure type is relatively rigid, with moderately high m.p.s [189–191 (1), 146–148 (2), 245–247 (3), and 147° (4)] and low density, and yet the tubes are lined only with the hydrogen atoms of the saturated hydrocarbon. The hydrogen bonding of the spines is fully shielded from the guest cavities, and therefore it is conceivable that protic guest molecules could diffuse into intact tubes without disruption of the host structure.

The long-known inclusion complexes formed by urea (or thiourea) with straight-chain hydrocarbon guests show some crystallographic similarity to the helical tubular diol structure, in that hexagonal tubes extend along six-fold screw axes, and the host molecules radiate from parallel three-fold screw axes in

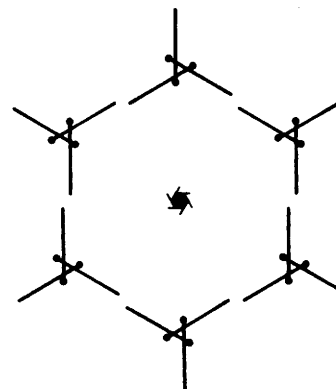


Figure 3. Schematic projection along the *c* axis of the host crystal structure for urea (and thiourea) inclusion complexes. The lines represent vertically planar host molecules, with their O (S) atoms close to three-fold screw axes. All hydrogen bonding occurs within the walls of the hexagonal prisms

hexagonal array.¹⁵ As shown schematically in Figure 3 the host cavity is hexagonal prismatic and the planar urea molecules are virtually parallel to the prism axis. However, the hydrogen-bonding schemes for the urea and the diol structure types are totally different. Each urea molecule engages four donor ($2 \times \text{NH}_2$) and four acceptor (to O) hydrogen bonds (twice the number per host diol), and all these hydrogen bonds occur in the vertical planes formed by the urea molecules in the walls of the prismatic cavity. This is quite dissimilar to the localised hydrogen-bonding spines which maintain the diol structure.

There are two significant consequences of these differences. One is that the hydrogen bonds of the urea structure are exposed to the guest species, while the spines of the diol structure are fully sequestered. The other is that the urea host structure is essentially invariant in dimensions, and (other than the minor expansion afforded by thiourea) not susceptible to geometrical modification by substitution of the host molecule because such substitution prevents the essential hydrogen bonding.

We have described the variations of tube size and shape that can be effected by modification of the bridges of the diol host molecules. A further variable in this helical tubular structure type is the length of the separation of the two OH functions, a distance which is virtually constant in the series reported here. With designed increase of this separation, through expansion of the polycyclic hydrocarbon core supporting the OH groups, it might be possible to increase the dimensions of the tube. One question that arises then is how far this expansion (and concomitant reduction in host density) can be continued without reversion to a different crystal structure type. In the following paper we analyse in detail the helical tubular crystal structures reported here, in order to elucidate the reasons for the variations in tube size and shape, and also to determine the necessary geometrical properties for host molecules adopting this crystal structure. Continuing investigations encompass the preparation and crystallographic characterisation of related diol molecules, and the inclusion of guest species by diols (1)—(4).

Acknowledgements

This research is supported by the Australian Research Grants Scheme. We thank Dr. J. J. Brophy and Mr. D. Nelson for

recording the mass spectra, and Mrs. H. Stender for recording the n.m.r. data.

References

- 1 R. Bishop and I. G. Dance, *J. Chem. Soc., Chem. Commun.*, 1979, 992.
- 2 R. Bishop, S. Choudhury, and I. G. Dance, *J. Chem. Soc., Perkin Trans. 2*, 1982, 1159.
- 3 D. D. MacNicol, J. J. McKendrick, and D. R. Wilson, *Chem. Soc. Rev.*, 1978, 7, 65.
- 4 R. Bishop, I. G. Dance, S. C. Hawkins, and T. Lipari, *J. Incl. Phenom.*, 1984, 2, 75.
- 5 J. Jacques, A. Collet, and S. H. Wilen, 'Enantiomers, Racemates and Resolutions,' Wiley, New York, 1981, ch. 2.2.
- 6 R. Bishop, I. G. Dance, and S. C. Hawkins, *J. Chem. Soc., Chem. Commun.*, 1983, 889.
- 7 I. G. Dance, R. Bishop, and M. L. Scudder, following paper.
- 8 R. Bishop and A. E. Landers, *Aust. J. Chem.*, 1979, 32, 2675.
- 9 H. C. Brown and P. J. Geoghegan, *J. Org. Chem.*, 1970, 35, 1844.
- 10 H. Meerwein and W. Schurmann, *Justus Liebig's Ann. Chem.*, 1913, 398, 196.
- 11 B. R. Vogt, *Tetrahedron Lett.*, 1968, 1579.
- 12 R. Greenwald, M. Chaykovsky, and E. J. Corey, *J. Org. Chem.*, 1963, 28, 1128.
- 13 S. C. Hawkins, unpublished results.
- 14 D. Nelson (U.N.S.W.), personal communication.
- 15 A. E. Smith, *Acta Crystallogr.*, 1952, 5, 224.

Received 3rd September 1985; Paper 5/1510